2008

Measurement of ep→epπ0 Beam Spin Asymmetries Above the Resonance Region

CLAS Collaborative

M. J. Amaryan
Old Dominion University, mamaryan@odu.edu

H. Bagdasaryan
Old Dominion University

S. Bültmann
Old Dominion University, sbueltma@odu.edu

S. L. Careccia
Old Dominion University

See next page for additional authors

Repository Citation

CLAS Collaborative; Amaryan, M. J.; Bagdasaryan, H.; Bültmann, S.; Careccia, S. L.; Dharmawardane, K. V.; Dodge, G. E.; Gavalian, G.; Guler, N.; Hyde-Wright, C. E.; Kalantarians, N.; Klien, A.; Klimenko, A. V.; Kuhn, S. E.; Niroula, M. R.; Tkachenko, S.; Weinstein, L. B.; and Zhang, J., "Measurement of ep→epπ0 Beam Spin Asymmetries Above the Resonance Region" (2008). *Physics Faculty Publications*. 378.
https://digitalcommons.odu.edu/physics_fac_pubs/378

Original Publication Citation

Collaboration, C., Masi, R. D., Garçon, M., Zhao, B., Amaryan, M. J., Ambrozewicz, P., . . . Zhao, Z. W. (2008). Measurement of ep→epπ0 beam spin asymmetries above the resonance region. *Physical Review C, 77*(4), 042201. doi:10.1103/PhysRevC.77.042201

Authors
CLAS Collaborative, M. J. Amaryan, H. Bagdasaryan, S. Bültmann, S. L. Careccia, K. V. Dharmawardane, G. E. Dodge, G. Gavalian, N. Guler, C. E. Hyde-Wright, N. Kalantarians, A. Klien, A. V. Klimenko, S. E. Kuhn, M. R. Niroula, S. Tkachenko, L. B. Weinstein, and J. Zhang

PHYSICAL REVIEW C **77**, 042201(R) (2008)

Measurement of $ep \to ep\pi^0$ beam spin asymmetries above the resonance region

R. De Masi,[1,30] M. Garçon,[1] B. Zhao,[2] M. J. Amaryan,[29] P. Ambrozewicz,[12] M. Anghinolfi,[18] G. Asryan,[40] H. Avakian,[35] H. Bagdasaryan,[29] N. Baillie,[39] J. Ball,[1] J. P. Ball,[4] N. A. Baltzell,[34] V. Batourine,[23] M. Battaglieri,[18] I. Bedlinskiy,[19] M. Bellis,[7] N. Benmouna,[14] B. L. Berman,[14] P. Bertin,[20,35] A. S. Biselli,[7,11] L. Blaszczyk,[13] S. Bouchigny,[30] S. Boiarinov,[35] R. Bradford,[7] D. Branford,[10] W. J. Briscoe,[14] W. K. Brooks,[35] S. Bültmann,[29] V. D. Burkert,[35] C. Butuceanu,[39] J. R. Calarco,[26] S. L. Careccia,[29] D. S. Carman,[35] L. Casey,[8] S. Chen,[13] L. Cheng,[8] P. L. Cole,[16] P. Collins,[4] P. Coltharp,[13] D. Crabb,[38] V. Crede,[13] N. Dashyan,[40] E. De Sanctis,[17] R. De Vita,[18] P. V. Degtyarenko,[35] A. Deur,[35] K. V. Dharmawardane,[29] R. Dickson,[7] C. Djalali,[34] G. E. Dodge,[29] J. Donnelly,[15] D. Doughty,[9,35] M. Dugger,[4] O. P. Dzyubak,[34] H. Egiyan,[35] K. S. Egiyan,[40] L. El Fassi,[3] L. Elouadrhiri,[35] P. Eugenio,[13] G. Fedotov,[25] G. Feldman,[14] A. Fradi,[30] H. Funsten,[39] G. Gavalian,[29] G. P. Gilfoyle,[33] K. L. Giovanetti,[22] F. X. Girod,[1,35] J. T. Goetz,[5] A. Gonenc,[12] R. W. Gothe,[34] K. A. Griffioen,[39] M. Guidal,[30] N. Guler,[29] L. Guo,[35] V. Gyurjyan,[35] K. Hafidi,[3] H. Hakobyan,[40] C. Hanretty,[13] F. W. Hersman,[26] K. Hicks,[28] I. Hleiqawi,[28] M. Holtrop,[26] C. E. Hyde-Wright,[29] Y. Ilieva,[14] D. G. Ireland,[15] B. S. Ishkhanov,[25] E. L. Isupov,[25] M. M. Ito,[35] D. Jenkins,[37] H. S. Jo,[30] J. R. Johnstone,[15] K. Joo,[2] H. G. Juengst,[14,29] N. Kalantarians,[29] J. D. Kellie,[15] M. Khandaker,[27] W. Kim,[23] A. Klein,[29] F. J. Klein,[8] A. V. Klimenko,[29] M. Kossov,[19] Z. Krahn,[7] L. H. Kramer,[12,35] V. Kubarovsky,[31,35] J. Kuhn,[7] S. E. Kuhn,[29] S. V. Kuleshov,[19] J. Lachniet,[7,29] J. M. Laget,[35] J. Langheinrich,[34] D. Lawrence,[24] T. Lee,[26] K. Livingston,[15] H. Y. Lu,[34] M. MacCormick,[30] N. Markov,[2] P. Mattione,[32] M. Mazouz,[21] B. McKinnon,[15] B. A. Mecking,[35] M. D. Mestayer,[35] C. A. Meyer,[7] T. Mibe,[28] B. Michel,[20] K. Mikhailov,[19] M. Mirazita,[17] R. Miskimen,[24] V. Mokeev,[25,35] B. Moreno,[30] K. Moriya,[7] S. A. Morrow,[1,30] M. Moteabbed,[12] E. Munevar,[14] G. S. Mutchler,[32] P. Nadel-Turonski,[14] R. Nasseripour,[12,34] S. Niccolai,[30] G. Niculescu,[22] I. Niculescu,[22] B. B. Niczyporuk,[35] M. R. Niroula,[29] R. A. Niyazov,[35] M. Nozar,[35] M. Osipenko,[18,25] A. I. Ostrovidov,[13] K. Park,[23] E. Pasyuk,[4] C. Paterson,[15] S. Anefalos Pereira,[17] J. Pierce,[38] N. Pivnyuk,[19] D. Pocanic,[38] O. Pogorelko,[19] S. Pozdniakov,[19] J. W. Price,[6] S. Procureur,[1] Y. Prok,[35,38] D. Protopopescu,[15] B. A. Raue,[12,35] G. Ricco,[18] M. Ripani,[18] B. G. Ritchie,[4] F. Ronchetti,[17] G. Rosner,[15] P. Rossi,[17] F. Sabatié,[1] J. Salamanca,[16] C. Salgado,[27] J. P. Santoro,[8] V. Sapunenko,[35] R. A. Schumacher,[7] V. S. Serov,[19] Y. G. Sharabian,[35] D. Sharov,[25] N. V. Shvedunov,[25] E. S. Smith,[35] L. C. Smith,[38] D. I. Sober,[8] D. Sokhan,[10] A. Stavinsky,[19] S. Stepanyan,[35] S. S. Stepanyan,[23] B. E. Stokes,[13] P. Stoler,[31] I. I. Strakovsky,[14] S. Strauch,[14,34] M. Taiuti,[18] D. J. Tedeschi,[34] A. Tkabladze,[14,28] S. Tkachenko,[29] C. Tur,[34] M. Ungaro,[2] M. F. Vineyard,[36] A. V. Vlassov,[19] E. Voutier,[21] D. P. Watts,[15] L. B. Weinstein,[29] D. P. Weygand,[35] M. Williams,[7] E. Wolin,[35] M. H. Wood,[34] A. Yegneswaran,[35] L. Zana,[26] J. Zhang,[29] and Z. W. Zhao[34]

(CLAS Collaboration)

[1]*CEA-Saclay, Service de Physique Nucléaire, F-91191 Gif-sur-Yvette, France*
[2]*University of Connecticut, Storrs, Connecticut 06269, USA*
[3]*Argonne National Laboratory, Argonne, Illinois 60439, USA*
[4]*Arizona State University, Tempe, Arizona 85287-1504, USA*
[5]*University of California at Los Angeles, Los Angeles, California 90095-1547, USA*
[6]*California State University, Dominguez Hills, Carson, California 90747, USA*
[7]*Carnegie Mellon University, Pittsburgh, Pennsylvania 15213, USA*
[8]*Catholic University of America, Washington, D. C. 20064, USA*
[9]*Christopher Newport University, Newport News, Virginia 23606, USA*
[10]*Edinburgh University, Edinburgh EH9 3JZ, United Kingdom*
[11]*Fairfield University, Fairfield, Connecticut 06824, USA*
[12]*Florida International University, Miami, Florida 33199, USA*
[13]*Florida State University, Tallahassee, Florida 32306, USA*
[14]*The George Washington University, Washington, D. C. 20052, USA*
[15]*University of Glasgow, Glasgow G12 8QQ, United Kingdom*
[16]*Idaho State University, Pocatello, Idaho 83209, USA*
[17]*INFN, Laboratori Nazionali di Frascati, I-00044 Frascati, Italy*
[18]*INFN, Sezione di Genova, I-16146 Genova, Italy*
[19]*Institute of Theoretical and Experimental Physics, Moscow RU-117259, Russia*
[20]*LPC Clermont-Ferrand, Université Blaise Pascal, CNRS/IN2P3, F-63177 Aubière, France*
[21]*LPSC, Université Joseph Fourier, CNRS/IN2P3, INPG, F-38026 Grenoble, France*
[22]*James Madison University, Harrisonburg, Virginia 22807, USA*
[23]*Kyungpook National University, Daegu 702-701, South Korea*
[24]*University of Massachusetts, Amherst, Massachusetts 01003, USA*
[25]*Moscow State University, General Nuclear Physics Institute, RU-119899 Moscow, Russia*
[26]*University of New Hampshire, Durham, New Hampshire 03824-3568, USA*
[27]*Norfolk State University, Norfolk, Virginia 23504, USA*
[28]*Ohio University, Athens, Ohio 45701, USA*
[29]*Old Dominion University, Norfolk, Virginia 23529, USA*

[30]*Institut de Physique Nucléaire, F-91406 Orsay, France*
[31]*Rensselaer Polytechnic Institute, Troy, New York 12180-3590, USA*
[32]*Rice University, Houston, Texas 77005-1892, USA*
[33]*University of Richmond, Richmond, Virginia 23173, USA*
[34]*University of South Carolina, Columbia, South Carolina 29208, USA*
[35]*Thomas Jefferson National Accelerator Facility, Newport News, Virginia 23606, USA*
[36]*Union College, Schenectady, New York 12308, USA*
[37]*Virginia Polytechnic Institute and State University, Blacksburg, Virginia 24061-0435, USA*
[38]*University of Virginia, Charlottesville, Virginia 22901, USA*
[39]*College of William and Mary, Williamsburg, Virginia 23187-8795, USA*
[40]*Yerevan Physics Institute, 375036 Yerevan, Armenia*
(Received 4 December 2007; published 14 April 2008)

The beam spin asymmetry (BSA) in the exclusive reaction $\vec{e}p \to ep\pi^0$ was measured with the CEBAF 5.77 GeV polarized electron beam and Large Acceptance Spectrometer (CLAS). The x_B, Q^2, t, and ϕ dependences of the π^0 BSA are presented in the deep inelastic regime. The asymmetries are fitted with a $\sin\phi$ function and their amplitudes are extracted. Overall, they are of the order of 0.04–0.11 and roughly independent of t. This is the signature of a nonzero longitudinal-transverse interference. The implications concerning the applicability of a formalism based on generalized parton distributions, as well as the extension of a Regge formalism at high photon virtualities, are discussed.

DOI: 10.1103/PhysRevC.77.042201 PACS number(s): 12.40.Vv, 13.40.Gp, 13.60.Hb, 13.60.Le

Introduction. Deeply virtual exclusive reactions $\gamma^* N \to N\gamma, N\pi, N\rho \cdots$, where the γ^* virtuality Q^2 is large, have the potential to probe nucleon structure at the parton level, as described by generalized parton distributions (GPDs). These distributions are universal functions that parametrize the nonperturbative structure of the nucleon. They include as limiting cases form factors and parton distributions, and they also provide access to hitherto unknown observables like the spatial distribution of partons of given longitudinal momentum fraction or the angular momentum of quarks and gluons inside the nucleon [1–3]. The description of deeply virtual meson production in terms of GPDs relies on a factorization theorem [4], which applies when the virtual photon γ^* is longitudinally polarized. In other words, meson production is expected to proceed mostly through longitudinal virtual photons in the Bjorken regime ($Q^2 \to \infty$ and the Bjorken variable x_B finite). The corresponding leading-twist diagram (or handbag diagram, illustrated in Fig. 1) for π^0 production is sensitive to specific flavor combinations of quark-helicity dependent (or "polarized") GPDs: $\frac{2}{3}\tilde{H}^u + \frac{1}{3}\tilde{H}^d$ and $\frac{2}{3}\tilde{E}^u + \frac{1}{3}\tilde{E}^d$ [3]. The $\tilde{H}^q$ are partly constrained by the polarized parton distributions Δq, while the $\tilde{E}^q$, largely unknown, are often modeled by a pion-pole term, which would not contribute to the $ep \to ep\pi^0$ process [3]. The Q^2 range in which the handbag diagram dominates, or where its contribution can be safely extracted, is not yet known for meson production.

An alternative description of exclusive meson production is based on Regge models, where trajectories are exchanged in the t channel as mediators of the interaction. While extensively studied for photoproduction [5], i.e., for $Q^2 = 0$ and transverse photons, the extension and applicability to virtual photons has not yet been considered in the specific case of neutral pion production.

So, two theoretical descriptions are *a priori* possible. The Regge approach starts from $Q^2 = 0$ and must be extended to nonzero Q^2, while the GPD approach has a firm QCD foundation in the Bjorken regime and its applicability must be tested at finite values of Q^2.

On the experimental side, while the focus has recently been on the production of real photons [6] (the so-called deeply virtual Compton scattering process, or DVCS) and of vector mesons [7–9], there is essentially no experimental data available on neutral pseudoscalar meson production above the resonance region. Cross sections were measured at DESY [10] at low values of Q^2, while a first result on the target spin asymmetry was obtained at CLAS [11]. For recent data on charged pion electroproduction in this kinematic regime, see Refs. [12] and [13].

The $ep \to ep\pi^0$ observables depend on the Q^2 and x_B variables, on the squared four-momentum transfer t to the proton, and on the angle ϕ between the leptonic and hadronic planes. The polarization of the exchanged virtual photon may be transverse (T) or longitudinal (L). It induces an azimuthal dependence of the reduced cross section for the $\gamma^* p \to p\pi^0$ process. For each (x_B, Q^2, t), taking the ratio of the difference over the sum of cross sections for opposite beam helicities, the beam spin asymmetry (BSA) has the following ϕ dependence:

$$A = \frac{\overrightarrow{\sigma} - \overleftarrow{\sigma}}{\overrightarrow{\sigma} + \overleftarrow{\sigma}} = \frac{\alpha \sin\phi}{1 + \beta\cos\phi + \gamma\cos 2\phi}. \quad (1)$$

The parameter α is proportional to a term denoted $\sigma_{LT'}$, originating from the imaginary part of an interference between the helicity amplitudes describing the process [14].

$$\alpha = \frac{\sqrt{2\epsilon(1-\epsilon)}\sigma_{LT'}}{\sigma_T + \epsilon\sigma_L}, \quad (2)$$

where σ_T and σ_L are the pure transverse and longitudinal cross sections, and ϵ is the usual virtual photon polarization parameter. Any measurement of a nonzero BSA would be indicative of an L-T interference, and therefore of contributions

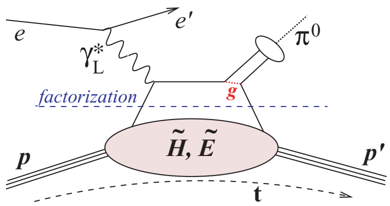

FIG. 1. (Color online) Schematic representation of the handbag diagram for neutral pion production. The symbol g stands for a gluon exchange between quark lines.

that cannot be described in terms of GPDs. Indeed, earlier but limited CLAS data indicated sizable BSA both for exclusive π^+ and π^0 production at large Q^2 [15].

Experiment and data analysis. This experiment used the CEBAF 5.77 GeV longitudinally polarized electron beam impinging on a 2.5-cm-long liquid-hydrogen target. The beam helicity was switched pseudorandomly at a frequency of 30 Hz, and the beam polarization, measured with a Møller polarimeter, had an average value of 79.4%. All final-state particles from the reaction $ep \to ep\pi^0$ followed by the decay $\pi^0 \to \gamma\gamma$ were detected. The six-sector CLAS spectrometer [16] was used to detect scattered electrons, recoil protons, and photons emitted at large angles. An additional small electromagnetic calorimeter ensured photon detection in the near forward region (4.5–15°). This inner calorimeter (IC) was built of 424 tapered lead-tungstate crystals, read out with avalanche photodiodes. It was calibrated using the two-photon decay of (inclusively produced) neutral pions.

Events were selected if an electron had generated a trigger, one and only one proton was identified, and any number of photons (above an energy threshold of 150 MeV) were detected in either the IC or the standard CLAS calorimeter EC [17]. Electrons were identified through signals in the EC and in the Čerenkov counters. Events considered hereafter included the kinematic requirements : $Q^2 > 1$ GeV^2, $\gamma^* p$ invariant mass $W > 2$ GeV, and scattered electron energy $E' > 0.8$ GeV. Protons were unambiguously identified over the whole momentum range of interest using time-of-flight from the target to the CLAS scintillators, as well as the track length and momentum determined by the drift chambers. A cut at $\pm 3\sigma$ was applied around the pion mass in the squared missing mass MM$^2(ep \to epX)$ distribution to exclude multipion background.

All clusters detected in the IC were assumed to originate from photons, while additional time-of-flight information was used in the EC to separate photons from neutrons. Photons hitting the calorimeters' edges were excluded. In addition, because the most forward hits in the IC had a sizable probability of originating from Møller accidental coincidences, a minimal angle was imposed on all photon candidates: $\theta_\gamma > 8^\circ - 0.75^\circ \times (E_\gamma/1\ \text{GeV})$.

To reconstruct the π^0 candidates, the two most energetic detected photons were considered, originating from either calorimeter. Four combinations were then possible: IC-IC, IC-EC, EC-IC, and EC-EC, where the photon with the highest energy was in the first mentioned calorimeter. The two calorimeters (IC and EC) had similar angular resolutions (about 4 mrad for 1 GeV photons) but different energy resolutions ($\sigma_{E_\gamma}/E_\gamma \simeq 4.5\%$ for IC and 11.6% for EC). When considering photon pairs, the kinematic cuts described below depended then on the four possible photon configurations defined previously.

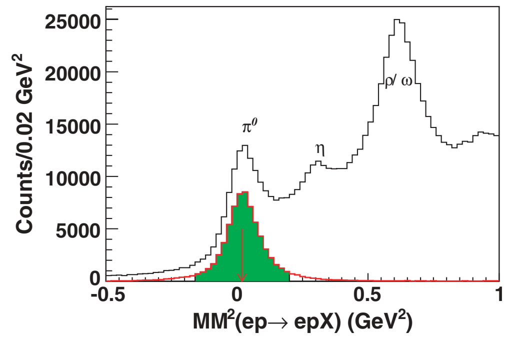

FIG. 2. (Color online) Distribution of squared missing mass for the $ep \to epX$ reaction before (black line) and after (thick red line) all cuts on other variables are applied. The arrow points to the pion mass, while the shaded green area corresponds to the selected events.

Events were then selected using a cut at $\pm 3\sigma$ in the squared missing mass MM$^2(ep \to e\pi^0 X)$ and a cut in the cone angle between the expected direction of the pion from $ep \to epX$ kinematics and the measured direction of the two-photon system. This selection resulted in very clean peaks in all kinematic correlations (Fig. 2 gives one example) and in the distributions of the two-photon invariant mass (see Fig. 3), with, respectively, 191K, 12K, 7K, and 14K events. The small remaining background was estimated using side-bands on the two-photon invariant mass spectra, for each beam helicity state and for each of the elementary bins in (x_B, Q^2, t, and ϕ).

π^0 *asymmetry.* The data were divided into 13 bins in the (x_B, Q^2) plane (see Fig. 4), 5 bins in $-t$ (defined by the bin limits 0.09, 0.2, 0.4, 0.6, 1, and 1.8 GeV^2), and 12 30° bins in ϕ. The resolutions in all corresponding variables were smaller than the bin sizes. Bin centering corrections were applied.

Within statistical accuracy, the ϕ distributions were found to be compatible with $A \simeq \alpha \sin\phi$ in each t bin (Fig. 4, right). The same compatibility was observed when the ϕ distributions were integrated in t. The determination of the asymmetry amplitude at 90° was stable whether the terms in $\cos\phi$ and $\cos 2\phi$ in Eq. (1) were included in the fit or not. Figure 5 gives the values of α in the 62 (x_B, Q^2, t) bins considered. By conservation of angular momentum, the helicity-flip transverse amplitude, and thus A and α, is identically zero as t reaches its kinematic limit t_0, corresponding to π^0s emitted in the direction of the virtual photon. At small x_B, the value of $-t_0$ is smaller than our first bin limit 0.09 GeV^2 (corresponding to the proton-energy detection threshold), which is why A does not go to zero. The increase of $-t_0$ explains the missing t bins at large x_B.

Systematic uncertainties arise from the event selection, as well as from the choice of the fit function used to extract α. Together, they were estimated at 0.016. The comparison between two separate analyses led to the increase of this value for two points in Fig. 5. Small compared to the systematic and statistical uncertainties, radiative corrections were neglected. The beam polarization measurements induce an additional

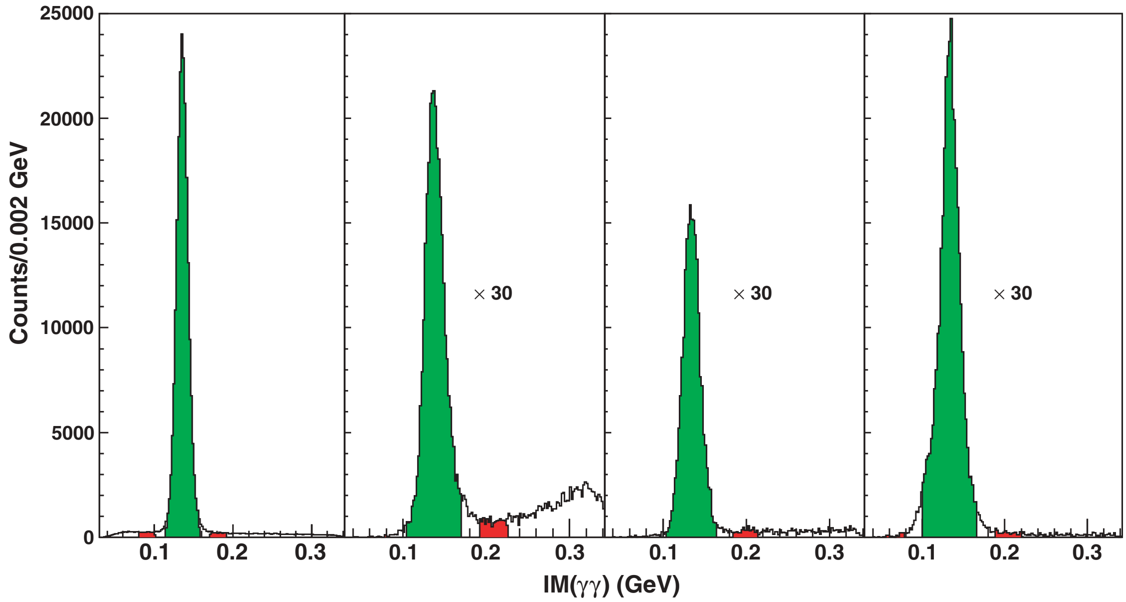

FIG. 3. (Color online) Distributions of the two-photon invariant mass, after the application of all cuts described in the text, for the four configurations IC-IC, IC-EC, EC-IC, and EC-EC, from left to right. The shaded areas correspond to the selected peaks (in green) and to the side-bands used in the background subtraction (in red). Note the change of scale for the last three configurations.

overall relative uncertainty of 3.5%. The data set may be found in Ref. [18].

Discussion of results. As seen in Fig. 5, the measured beam spin asymmetries are systematically of the order of 0.04 to 0.11, over a wide kinematic range in x_B, Q^2, and t. In particular, there is no evidence of a decrease of $\alpha(t)$ as a function of Q^2. This is a clear sign of a nonzero LT' interference among the amplitudes describing the $\gamma^* p \to p\pi^0$ reaction.

In the GPD formalism, only the longitudinal amplitude, dominant in the Bjorken regime, is calculated. The present evidence of nonzero transverse terms indicates that it may be necessary to perform a L/T separation to isolate the longitudinal part of the cross section.

A Regge-type model (JML) describes the pion photo- and electroproduction according to the diagrams in Fig. 6. The model parameters are tuned to describe the photoproduction data. In particular the strength of the b_1 exchange term is adjusted to reproduce the linearly polarized photon beam asymmetry [5]. In extending the model to the case of electroproduction, vertex electromagnetic form factors are adjusted to reproduce the DESY data [10]. The application to the kinematic range of the present data is then an extrapolation of the model, which will be fully described elsewhere [19] and reproduces the target spin asymmetry [11]. When considering the pole terms, only the b_1 exchange, through its interference with the ρ and ω exchanges (because of opposite parities), may generate a nonzero beam spin asymmetry. Treating the box diagrams in the approximation of on-shell intermediate particles yields the solid curves presented in Figs. 4 and 5. As apparent in Fig. 4, the model generates sizable γ and β terms in Eq. (1), corresponding, respectively, to a TT interference due to the pole terms of Fig. 6(a) and to an LT interference due to the box diagrams of Fig. 6(c).

Summary. Sizeable beam spin asymmetries for exclusive neutral pion electroproduction of the proton have been

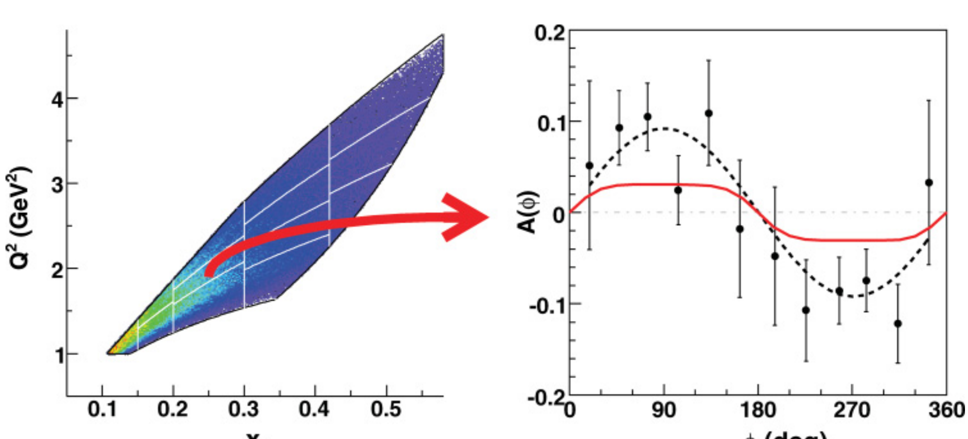

FIG. 4. (Color online) (Left) Kinematic coverage and binning in the (x_B, Q^2) plane. (Right) $A(\phi)$ for one of the 13 (x_B, Q^2) bins and one of the 5 bins in t, corresponding to $\langle x_B\rangle = 0.249$, $\langle Q^2\rangle = 1.95$ GeV^2, and $\langle t\rangle = -0.29$ GeV^2; the black dashed curve corresponds to a fit with $A \simeq \alpha \sin\phi$ and the red solid curve to the JML model discussed in the text.

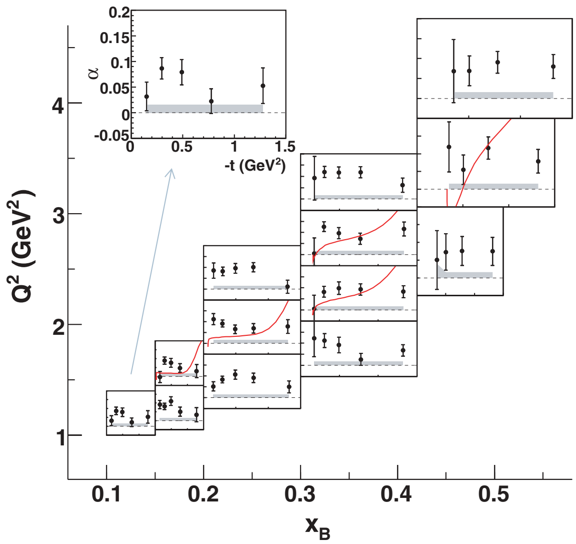

FIG. 5. (Color online) Fit parameter α, as extracted from $A \simeq \alpha \sin\phi$, as a function of $-t$. The location of each individual plot corresponds to the approximate coverage in (x_B, Q^2), except the upper left one (an enlargement of the lower left one), which indicates the scales common to all plots. The grey areas indicate the maximal size of systematic uncertainties. For selected kinematics, the red curves correspond to the JML model discussed in the text.

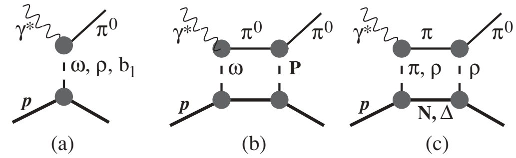

FIG. 6. Diagrams describing the neutral pion production in the JML model. (a) Pole terms. (b) Box diagram with elastic π^0 rescattering. (c) Box diagram with charge exchange ($\pi^+N, \pi^+\Delta^0$, and $\pi^-\Delta^{++}$ are the three intermediate states considered). The exchanged mesons are to be understood as the corresponding Regge trajectories, and **P** stands for the Pomeron.

measured above the resonance region for the first time. These nonzero asymmetries imply that both transverse and longitudinal amplitudes participate in the process. The determination of the longitudinal cross section in the kinematic regime considered here, and the subsequent extraction of polarized generalized parton distributions, may then necessitate to perform an L/T separation. For the same purpose, measurements at still higher values of Q^2 would be crucial in providing evidence for the expected decrease of the transverse cross section. Presently, the only available model to calculate this observable is based on Regge theory. It reproduces the magnitude of the asymmetries at intermediate values of t, but does not exhibit the measured kinematic dependencies. Beam spin asymmetries for exclusive η electroproduction, as well as cross sections for π^0 and η meson production, will be considered in forthcoming publications.

We acknowledge the outstanding efforts of the staff of the Accelerator and Physics Divisions at JLab, as well as of the technical staff at DAPNIA-Saclay and IPN-Orsay, that made this experiment possible. This work was supported in part by the French Centre National de la Recherche Scientifique and Commissariat à l'Energie Atomique, the U.S. Department of Energy and National Science Foundation, the Italian Istituto Nazionale di Fisica Nucleare, the Korean Science and Engineering Foundation, and the U.K. Engineering and Physical Science Research Council. The Jefferson Science Associates (JSA) operates the Thomas Jefferson National Accelerator Facility for the United States Department of Energy under Contract DE-AC05-06OR23177.

[1] X.-D. Ji, Phys. Rev. Lett. **78**, 610 (1997).
[2] M. Burkardt, Phys. Rev. D **62**, 071503(R) (2000).
[3] M. Diehl, Phys. Rep. **388**, 41 (2003).
[4] J. C. Collins, L. Frankfurt, and M. Strikman, Phys. Rev. D **56**, 2982 (1997).
[5] M. Guidal, J. M. Laget, and M. Vanderhaeghen, Nucl. Phys. **A627**, 645 (1997).
[6] M. Garçon, AIP Conf. Proc. **870**, 93 (2006).
[7] A. Airapetian *et al.* (HERMES), Eur. Phys. J. C **17**, 389 (2000).
[8] C. Hadjidakis *et al.* (CLAS Collaboration), Phys. Lett. **B605**, 256 (2005).
[9] L. Morand *et al.* (CLAS Collaboration), Eur. Phys. J. A **24**, 445 (2005).
[10] F. Brasse *et al.*, Phys. Lett. **B58**, 467 (1975).
[11] S. Chen *et al.* (CLAS Collaboration), Phys. Rev. Lett. **97**, 072002 (2006).
[12] A. Airapetian *et al.* (HERMES Collaboration), Phys. Lett. **B659**, 492 (2008).
[13] T. Horn *et al.* (2007), arXiv:0707.1794[nucl-ex].
[14] D. Drechsel and L. Tiator, J. Phys. G **18**, 449 (1992).
[15] H. Avakian *et al.* (CLAS Collaboration), Phys. Part. Nucl. **35**, S114 (2004).
[16] B. A. Mecking *et al.* (CLAS Collaboration), Nucl. Instrum. Methods A **503**, 513 (2003).
[17] M. Amarian *et al.*, Nucl. Instrum. Methods A **460**, 239 (2001).
[18] CLAS Physics Data Base, http://clasweb.jlab.org/physicsdb/intro.html.
[19] J. M. Laget (in preparation).